Complex Behavior in Sigma-Delta Modulator

Cvetko D. Mitrovski

Abstract: **In this paper we investigate the dynamic behavior of a general class of second order single loop sigma delta modulators driven by a constant input. The proposed approach is based on nonlinear dynamic analysis of the piece wise linear model of the modulator.**

Keywords: **Sigma-delta modulator, trajectories, fractals, attractor, phase space.**

I. INTRODUCTION

The sigma delta modulation, as a method of analog to digital conversion has attracted much research interest since it was for the first time presented in 1962[1]. This technique is now finding widespread use in various signal processing applications, which is motivated by both, simplicity of the design and the fault tolerance to fabrication errors. The last two factors make the sigma delta modulators very suitable to integrated circuit applications.

The devices designed on the principle of sigma-delta modulation are non-linear systems which convert a time sampled analog signal to a stream of bits. Usually, they consists one or two integrators and a one bit quantiser in a feedback loop. In general, the basic structure could be modified by substituting the integrator(s) with any subsystem with low-pass or band-pass characteristics, while the other parts remain the same. This configuration can be generalized as a non-linearity within a feedback path, which is a classic route to complex behavior [2]. Therefore, the exact analyze of any sigma delta modulator is highly nontrivial.

In this paper we use nonlinear dynamic to discover the properties of a class of single loop second order modulators realized with an arbitrary band pass filter operating on the boundary of its stability region. This problem is actually generalization of the problem of band-pass sigma delta modulation analyzed in [3][4].

In this paper we first model the sigma delta modulator by piece wise linear model and after that we analyze the nature of its trajectories and their dependence on the parameters and the initial conditions. At the end we give some conclusions illustrated by our simulation results.

II. BASIC SIGMA–DELTA MODEL

The general structure of basic Sigma delta modulator consists of integrator and a one bit quantizer in a feedback loop. In general case, the integrator can be substituted by any subsystem with a properly chosen transfer function, as shown in Figure 1.

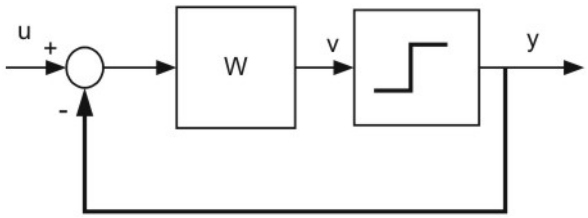

Figure 1. Block diagram of single loop sigma delta modulator

In our study we suppose that the integrator(s) is(are) substituted by the second order subsystem

$$W(z) = \frac{b_1 z^{-1} + b_0 z^{-2}}{1 - 2\cos(\theta) z^{-1} + z^{-2}}, \qquad (1)$$

where: b_1 and b_0 are arbitrary parameters and θ is the angle which determines the pole positions of W(z) on the unit circle. This model is an extension of the model analyzed in [4], in which the parameters b_1 and b_0 were chosen to be

$$b_1 = 2\cos(\theta); \quad b_0 = -1 \qquad (2)$$

The dynamic behavior of this model, can be described by the following system of difference equations

$$\begin{aligned} x_1(k+1) &= x_2(k) \\ x_2(k+1) &= 2\cos(\theta) x_2(k) - x_1(k) - f(.) \end{aligned} \qquad (3)$$

where:

$$\begin{aligned} f(.) = b_1 &\left(u(k) - \mathrm{sign}(x_2(k))\right) + \\ &+ b_0 \left(u(k-1) - sign(x_1(k))\right), \end{aligned} \qquad (4)$$

and $x_i(k)$, i=1,2 are the internal states of the modulator.

Table -1

i	Ri	$x_1(k)$	$x_2(k)=x_1(k+1)$	f(i)
0	R_0	$x_1(k)=0$	$x_2(k)=0$	$U(b_1+b_0)$
1	R_1	$x_1(k)>0$	$x_2(k)>0$	$U(b_1+b_0)-b_1-b_0$
2	R_2	$x_1(k)<0$	$x_2(k)>0$	$U(b_1+b_0)-b_1+b_0$
3	R_3	$x_1(k)<0$	$x_2(k)<0$	$U(b_1+b_0)+b_1+b_0$
4	R_4	$x_1(k)>0$	$x_2(k)<0$	$U(b_1+b_0)+b_1-b_0$
5	R_5	$x_1(k)=0$	$x_2(k)>0$	$U(b_1+b_0)-b_1$
6	R_6	$x_1(k)=0$	$x_2(k)<0$	$U(b_1+b_0)+b_1$
7	R_7	$x_1(k)<0$	$x_2(k)=0$	$U(b_1+b_0)+b_0$
8	R_8	$x_1(k)>0$	$x_2(k)=0$	$U(b_1+b_0)-b_0$

[1]Cvetko D. Mitrovski is with the Faculty of Technical Sciences, I.L.Ribar bb, 7000 Bitola, Macedonia, E-mail: cvetko.mitrovski @uklo.edu.mk

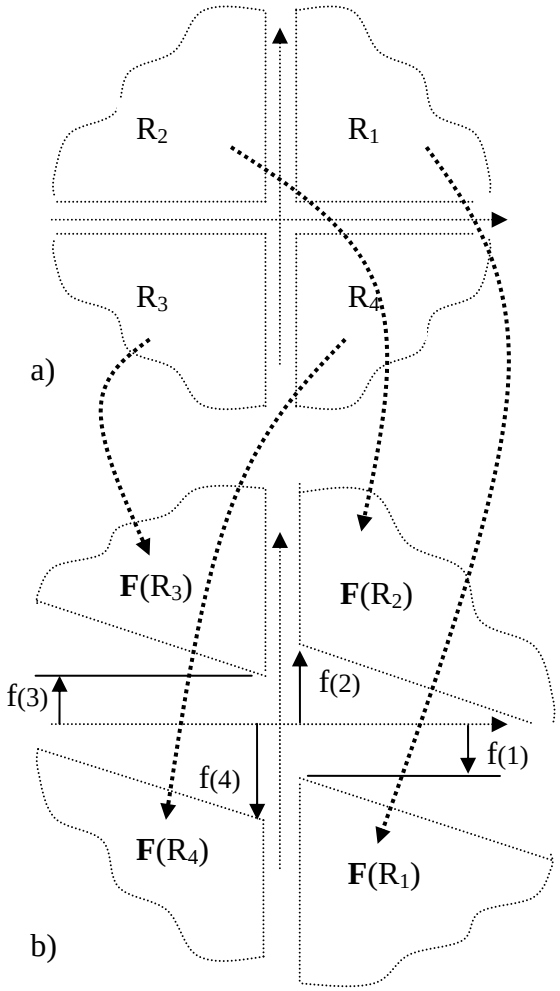

Figure-2. a) Regions of the phase space of the map b) Images of the regions R_i,i=1,2,3,4.

Since f(.) depends on the terms sign(x_2(k) and sign(x_1(k), in case of constant input u(k)=u(k-1)=U, its values will belong to a finite set of nine values given in the table 1.

III. Piece Wise Linear model

The above system can be modeled by the piecewise-linear map $\mathbf{F}(\mathbf{x}(k)): R^2 \rightarrow R^2$ defined by

$$\mathbf{x}(k+1) = \mathbf{A}\mathbf{x}(k) + \mathbf{b}s_i \quad \text{for } \mathbf{x}(\mathrm{k}) \in R_i \qquad (5)$$

where:

$$\mathbf{x}(k) = \begin{vmatrix} x_1(k) \\ x_2(k) \end{vmatrix}; \quad \mathbf{A} = \begin{vmatrix} 0 & 1 \\ -1 & 2\cos(\theta) \end{vmatrix}; \quad \mathbf{b} = \begin{vmatrix} 0 \\ 1 \end{vmatrix},$$

R_i, i=0,1,2,3,4,5,6,7,8 are disjoint subspaces that cover R^2 and s_i=f(i).

The matrix **A** is the Jacobian of the map and it has an unit module (|det(**A**)|=1) for any θ. Therefore, the transformation **A** is a rotation on an ellipse with center in origin (0, 0) and axis at $\pm\pi/4$.

According to this, each trajectory starting from any initial point will visit the regions R_i i=0,1,…,8 in some order by generating an infinite symbolic sequence "$s_0s_1…s_k…$" composed by the indexes of the visited regions. These symbolic sequences are generated by some patterns, which could be determined by analyzing the position of the images of the disjoint regions R_i, (**F**(R_i)), i = 0,1,2,..,8 and their originals.

In Figure-2 we have illustrated the transformations of the regions R_1, R_2 R_3 and R_4 by the map (5) while the transformation of the other regions (positive and negative parts of the axes Ox_1 and Ox_2) are not shown.

The relative position of the images of the regions **F**(R_i) depend on the parameters of the map. If b_0<0, then the regions **F**(R_1) and **F**(R_2) (**F**(R_3) and **F**(R_4) are overlapping while for b_0>0 they are not.

If **F**(R_1) and **F**(R_2) are overlapping, then the images of R_5, R_6, R_7 and R_8 satisfy the following relations:

$$\mathbf{F}(R_5) \subset \mathbf{F}(R_1) \cap \mathbf{F}(R_2) \qquad (6)$$

$$\mathbf{F}(R_6) \subset \mathbf{F}(R_3) \cap \mathbf{F}(R_4) \qquad (7)$$

$$\mathbf{F}(R_7) \cup \mathbf{F}(R_8) \subset R_5 \cup R_6 . \qquad (8)$$

Otherwise, **F**(R_5) (**F**(R_6)) is equidistant to the parallel sides of **F**(R_1) and **F**(R_2) (**F**(R_3) and **F**(R_4)).

By changing the parameter θ we modify the angle of open sectors **F**(R_i), i=1,2,3,4, while by changing of b_0, b_1 and U we influence on their vertical position in R^2 and on their relative position. With that, we influence on the map dynamics by modifying the transition patterns among the regions. Typical example for this is the transition from R_1 to R_1, which could be enabled or disabled by choosing the appropriate value for the corner points of **F**(R_1) below or above the x_1 axis.

IV. Unbounded trajectories

If b_0 >0 ($2b_0$=f(2)-f(1)=f(3)-f(4)) the images of the regions **F**(R_1) and **F**(R_2) (**F**(R_3) and **F**(R_4)) will not overlap. In that case any trajectory starting from any initial condition will diverge spirally toward infinity. This phenomenon is obvious when f(1)*f(2) <0 (f(3)*f(4) <0) because in that case, in each iteration, the shifting part of the map pushes the image toward the exterior of the ellipse.

If f(1)*f(2)>0 (f(3)*f(4) >0) the trajectories remain globally expanding, but they have some local contractions. The smaller the gap between **F**(R_1) and **F**(R_2) is, the more dominant local contractions are. In this case the trajectories while evolving in some regions are pushed, sometimes toward the interior of the ellipses and sometimes toward its exterior. Therefore the trajectories create curved ellipse like patterns which are appearing periodically in the phase space (Figure-3a). By increasing the value of b_0, the gap between **F**(R_1) and **F**(R_2) is increased and the intensity of the local contractions in the

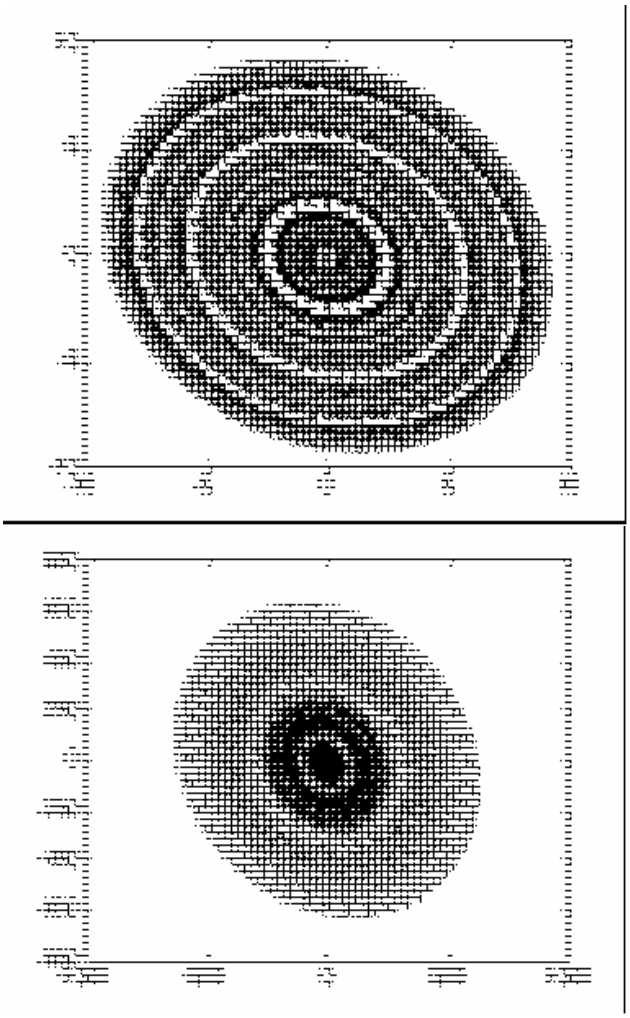

Figure 3 Expanding trajectories starting from **x**(0)=(0.00237, -0.0123) of the map with parameters θ=1.73, b_1=2*cos(1.73) a) and b_0=0.0001. b) b_0=0.05

expanding trajectories is reduced. That leads to elimination of the ellipse like curvatures in the expanding trajectories as illustrated in Figure 3b).

V. BOUNDED TRAJECTORIES

If b_0 (b_0<0) enables even a slightest overlapping of **F**(R_1) and **F**(R_2) (**F**(R_3) and **F**(R_4)), then the trajectories of the map (5) are bounded by an open concave eight corner polygon. In case of U=0, this polygon has a central symmetry.

No matter whether $U \neq 0$ or U=0, all the trajectories that start out of this polygon are trapped in it (after a certain number of iterations). Therefore we shall concentrate on the trajectories which are starting from the interior of this polygon and remain in it for all the time. While evolving, these trajectories also generate infinite symbolic sequences composed of the indexes of the visited regions.

If the generated symbolic sequence is periodic, then the trajectory is either periodic (finite set of points), or dense on a finite number of ellipses. If they are periodic, then the corresponding trajectories are fractal, and if they are eventually periodic, then the trajectories posses his irregular

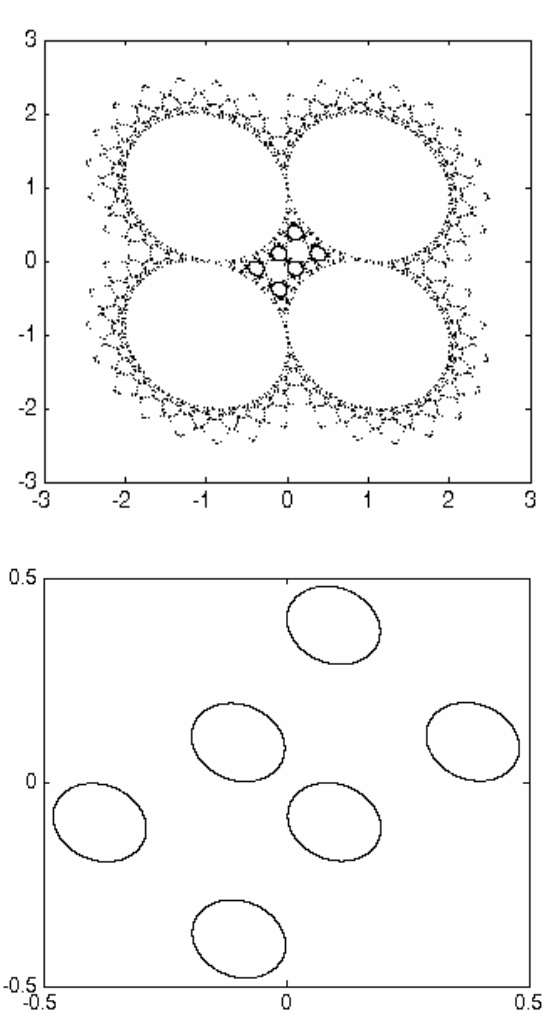

Figure 4. Bounded trajectory of the map U=0, θ =1.73, b_1 = 2*cos(θ), b_0 =-0.001 a) starting from **x**(0)=(0.00237, -0.0123) b) starting from **x**(0)=(0.00512, -0.0626).

part after which they are attracted either by a sets of fixed points or by a sets of dense ellipse like orbits.

The existence of various types of trajectories is illustrated in Figure-4 and Figure-5.

The trajectory shown in Figure-4a has irregular (fractal like) initial part which converges to a set of six small ellipses, while the trajectory starting from **x**(0)=(0.00512, -0.0626) remains on six dense ellipses.

In case when b_1 = 2*cos(θ) and b_0 =-1, the map (5) models the band-pass sigma delta modulator [4]. For this combination of parameters b_1 and b_0, the map generates all tree types of trajectories. In figure 5, we illustrate a fractal trajectory of this map, starting from **x**(0)=(0.016,-0.0485), which visits infinite number of ellipses. While evolving it shapes almost all the ellipse regions in the phase space from which only regular trajectories could be generated (sets of periodic points and sets of dense ellipses).

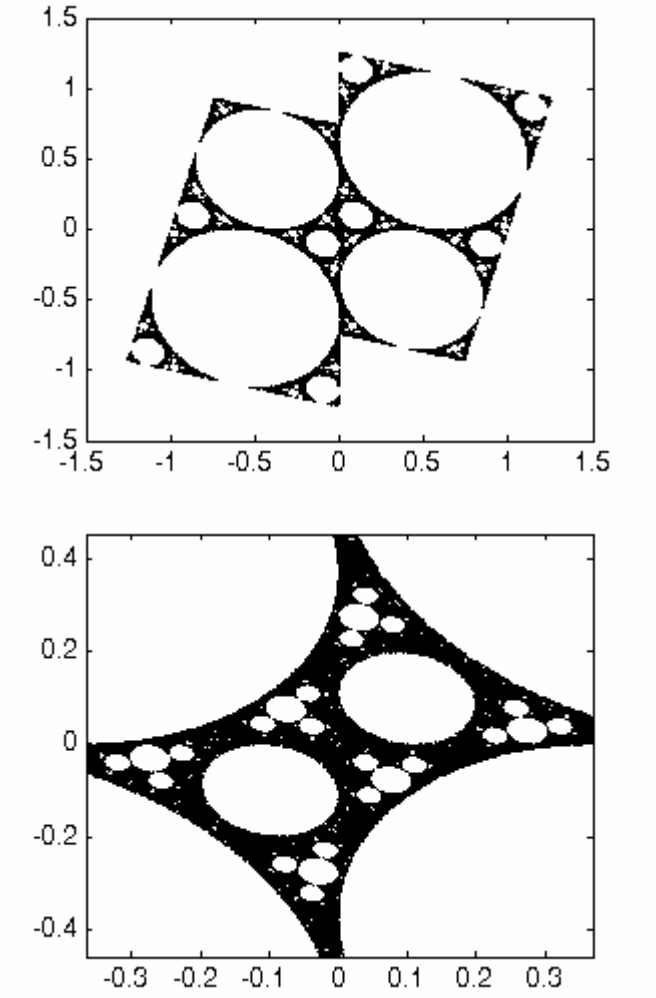

Figure 6. Fractal trajectory of the map U=0, θ =1.7, b_1 = 2*cos(θ), b_0 =-1 starting from **x**(0)=(0.016, -0.0485). b) Zoomed detail

So, for a constant input U we could obtain various symbolic sequences in dependence of the initial conditions. Since the symbolic sequence determines the bit stream output of the modeled sigma delta modulator, it means that we could have different, even false outputs.

VI. CONCLUSION

In this paper we have observed a wide class of constant input driven sigma delta modulators realized with a second order digital filter (operating on the boundary of its stability region) and one bit quantizer in a feedback loop. For this class of devices we have determined the piece wise liner map which describes its internal behavior. After that we have determined that the parameter b_0 determines the safe operation space.

In case when b_0 >0 the map exhibits unbounded trajectories which means that the modeled real sigma delta modulator could be damaged due to excessive internal dissipation. In cases when b_0<0, the map exhibits bounded trajectories which cannot damage the modeled device, but its complex behavior could lead to different and sometimes false output streams of the constant driven real device.

REFERENCES

[1] H. Inose, Y. Yasuda and J. Marakami, *"A telemetering system by code modulation, delta-sigma modulation,"* IRE Trans. on Space, Electronics and Telemetry, SET-8, pp. 204-209, Sept. 1962.

[2] L. O. Chua and T. Lin "Chaos in digital filters", *IEEE Trans. Circuits and Systems*, Vol 35 pp 648-658, June 1988.

[3] O. Feely and D. Fitzgerald "*Nonlinear Dynamics and Chaos in Sigma–Delta Modulation*", Journal of the Franklin institute, Vol 331B, pp 903-936, 1994.

[4] O. Feely and D. Fitzgerald "Band-pass Sigma-Delta Modulation –An Analysis From the Perspective of Nonlinear Dynamics", IEEE *J. Circuit Theory and Applications*, vol 18, pp 146-149, 1996.

[5] C.W. Wo and L. O. Chua "Symbolic dynamics of Piecewise-Linear Maps", *IEEE Trans. Circuits and Systems II,* Vol 41 pp 420-424, June 1994.